Daniel Ajona[1,2,3,4], Sergio Ortiz-Espinosa[1], Haritz Moreno[1,2], Teresa Lozano[2,5], María J Pajares[1,2,3,6], Jackeline Agorreta[1,2,3,6], Cristina Bértolo[1], Juan J Lasarte[2,5], Silvestre Vicent[1,2,6], Kai Hoehlig[7], Axel Vater[8], Fernando Lecanda[1,2,3], Luis M Montuenga[1,2,3,6], Ruben Pio[1,2,3,4]

Affiliations of authors: [1]University of Navarra, Center for Applied Medical Research (CIMA), Program in Solid Tumors and Biomarkers, Pamplona, Spain. [2]Navarra's Health Research Institute (IdiSNA), Pamplona, Spain. [3]Centro de Investigación Biomédica en Red de Cáncer (CIBERONC). [4]University of Navarra, School of Sciences, Department of Biochemistry and Genetics, Pamplona, Spain. [5]University of Navarra, CIMA, Program in Immunology and Immunotherapy, Pamplona, Spain. [6]University of Navarra, School of Medicine, Department of Histology and Pathology, Pamplona, Spain. [7]NOXXON Pharma, Berlin, Germany. [8]Aptarion biotech, Berlin, Germany.

Running head: Anti-PD-1 and anti-C5a combined immunotherapy in lung cancer

Keywords: PD-1, C5a, immunotherapy, combined therapy, complement system, lung cancer

Grant support: This work was supported by Foundation for Applied Medical Research (FIMA), Red Temática de Investigación Cooperativa en Cáncer (RD12/0036/0040), CIBERONC CB16/12/00443, Fondo de Investigación Sanitaria-Fondo Europeo de Desarrollo Regional (FEDER, PI13/00806, PI14/01686), Spanish Ministry of Economy and Competitiveness (SAF2013-46423-R and SAF2015-71606-R), and European Commission (618312 KRASmiR FP7-PEOPLE- 2013-CIG). S.V. is a fellow of the Ramón y Cajal Program (MICINN, RYC-2011- 09042). F.L. is funded by "la Caixa" Foundation and Caja Navarra Foundation.

Corresponding author: Ruben Pio. Program in Solid Tumors and Biomarkers. CIMA Building, Pio XII 55, 31008 Pamplona, Spain. E-mail: rpio@unav.es. Tel: +34 948194700. Fax: +34 948194714.

Disclosure of potential conflicts of interest: Axel Vater is founder of APTARION biotech, which holds intellectual property rights to certain anti-C5a L-aptamers, including AON-D21. The other authors declare no conflict of interest.

Statement of significance:

Using a variety of preclinical models of lung cancer, we demonstrate that the blockade of C5a results in a substantial improvement in the efficacy of anti-PD-1 antibodies against lung cancer growth and metastasis. This study provides the preclinical rationale for the combined blockade of PD-1/PD-L1 and C5a to restore antitumor immune responses, inhibit tumor cell growth, and improve lung cancer patient outcomes.

ABSTRACT

Disruption of the programmed cell death protein 1 (PD-1) pathway with immune checkpoint inhibitors represents a major breakthrough in the treatment of non-small cell lung cancer. We hypothesized that a combined inhibition of C5a/C5aR1 and PD-1 signaling may have an antitumor synergistic effect. RMP1-14 antibody was used to block PD-1 and an L-aptamer to inhibit signaling of complement C5a with its receptors. Using syngeneic models of lung cancer we demonstrate that the combination of C5a and PD-1 blockade markedly reduces tumor growth and metastasis, and leads to prolonged survival. This effect is accompanied by a negative association between the frequency of CD8 T cells and myeloid-derived suppressor cells (MDSCs) within the tumors, which may result in a more complete reversal of CD8 T-cell exhaustion. Our study provides support for the clinical evaluation of anti-PD-1 and anti-C5a drugs as a novel combination therapeutic strategy for lung cancer.

INTRODUCTION

Immunotherapy based on checkpoint inhibitors has emerged as a potent tool for the treatment of lung cancer, the leading cause of cancer death worldwide. Among the numerous immunotherapeutic strategies, monoclonal antibodies that inhibit the interaction between programmed death-1 (PD-1) and its ligands have shown the most compelling clinical results in lung cancer. Monoclonal antibodies raised against PD-1 have been approved by the FDA for patients with metastatic non-small cell lung cancer (1). By blocking PD-1, these drugs remove the inhibition of T-cell activation and restore antitumor immune responses. However, PD-1 inhibition is not capable of reversing all resistance mechanisms and a proportion of patients do not respond adequately to anti-PD-1 immunotherapies. Consequently, combination therapies, that block more than one immunomodulatory pathway, have been proposed to further enhance the antitumor efficacy of anti-PD-1 individual treatments (2).

A hallmark mechanism of synergy in immunotherapy is the reactivation of effector T cells together with the elimination of immunosuppressive cells, such as myeloid-derived suppressor cells (MDSCs) or regulatory T cells (Tregs). In this regard, PD-1/PD-L1 blockade is not able to reduce the T cell suppressive activity of the tumor microenvironment, which can be caused by the accumulation of MDSCs (3) or Tregs (4). Therefore, a successful reversal of the tumor immunosuppressive microenvironment represents a window of opportunity to overcome tumor resistance in cancer immunotherapy.

Anaphylatoxin C5a, an active proteolytic fragment released after activation of the complement system, contributes to lung cancer progression by promoting an immunosuppressive microenvironment in which MDSCs are involved (5,6). All pathways of complement, an essential part of innate immunity, converge in the cleavage and activation of the central components C3 and C5, which leads to the release of anaphylatoxins C3a and C5a. Although C5a is generally known to be a chemoattractant for pro-inflammatory leukocytes,

several studies have demonstrated a tumor-promoting role for this molecule and the idea of blocking complement for the treatment of cancer is gaining recognition (7). In mouse models of cancer, complement deficiencies and pharmacological blockade of complement-related mediators, including C5a, have been associated with impaired tumor growth (8). C5a is also able to modulate antitumor immunity by altering T cell responses in premetastatic niches (9). In the case of lung cancer, the expression of some immunosuppressive molecules is significantly reduced after blockade of the C5a receptor-1 (C5aR1) (5). Besides, C5aR1 blockade diminishes the percentage and activity of MDSCs in cancer models, including lung cancer (5,8,10). By studying C3 knockout mice, it has been recently shown that complement inhibits antitumor immunity through a PD-1 independent pathway (11). All these studies reveal the important role played by C5a/C5aR1 signaling in tumor immunity, and point to this pathway as a potential therapeutic target in the context of checkpoint inhibition.

In this study we have evaluated the therapeutic efficacy of the combined administration of anti-PD-1 and anti-C5a drugs in a variety of lung cancer models. From these experiments, we conclude that C5a blockade results in a more permissive environment for immune-mediated tumor rejection and, consequently, its combined administration with anti-PD-1 antibodies synergistically impairs lung cancer growth and metastasis.

RESULTS

C5aR1 genetic deficiency and C5a pharmacological blockade decreases lung tumor growth

To explore the role of C5a/C5aR1 signaling in lung cancer initiation and progression, we crossed C5aR1 deficient mice ($C5aR1^{+/-}$) to $Kras^{LSL\text{-}G12D/+}$ mice that develop lung adenocarcinomas by inducing the expression of oncogenic Kras upon intratracheal inoculation of Cre recombinase. Deletion of C5aR1 had a noticeable effect on mutant Kras-induced lung carcinogenesis (Fig. 1A). Thus, $Kras^{LSL\text{-}G12D/+}$;$C5aR1^{-/-}$ mice developed significantly smaller tumors compared to C5aR1 wild-type littermates, while no differences were observed in the total number of tumors (Fig. 1B). $Kras^{LSL\text{-}G12D/+}$;$C5aR1^{-/-}$ mice showed a reduced percentage of myeloid-derived suppressor cells (MDSCs) in their spleens (Fig. 1C). No differences were observed in the frequencies of CD4 T cells, CD8 T cells or Tregs (data not shown). Immunohistochemical analysis of the tumors showed an increase in CD3 cells from $Kras^{LSL\text{-}G12D/+}$;$C5aR1^{-/-}$ mice close to statistical significance (Fig. 1D). No differences were found in proliferation (Ki67), apoptosis (cleaved caspase-3) or angiogenesis (CD31) (data not shown). Using an independent mouse cohort, we observed that survival of $Kras^{LSLG12D/+}$;$C5aR1^{-/-}$ mice was significantly longer than that of $Kras^{LSL\text{-}G12D/+}$;$C5aR1^{+/+}$ littermates (Fig. 1E).

We next investigated the effect of the pharmacological blockade of C5a in a syngeneic mouse model based on the subcutaneous growth of 393P cells, a mouse model of Kras-driven lung adenocarcinoma (12). We used AON-D21 (formerly NOX-D21), an L-aptamer which tightly binds to both mouse and human C5a and efficiently inhibits the interaction with its receptors (Supplementary Results, Supplementary Fig. S1 and Supplementary Table S1 show information about the pharmacology and other characteristics of this molecule). AON-D21 treatment led to a partial reduction of tumor growth when compared to the effect of revAON-D21, a non-functional control L-aptamer (Fig. 1F). Analysis of splenocyte subpopulations

revealed a reduction in the percentage of MDSCs (Fig. 1G), with no significant differences in CD4 T cells, CD8 T cells or Tregs (data not shown). These genetic and pharmacological results demonstrate the influence of the C5a/C5aR1 pathway on lung tumor growth and the potential value of blocking C5a for the treatment of lung cancer.

C5a inhibition synergizes with PD-1 blockade to prevent lung cancer growth and metastasis

We postulated that an anti-C5a treatment may enhance the capacity of PD-1 blockade to control lung tumor growth. In the subcutaneous 393P model, the combination of the anti-C5a L-aptamer AON-D21 (every other day) with the anti-PD-1 monoclonal antibody RMP1-14 (days 7, 10 and 14) resulted in a significant reduction of tumor growth, as compared to the effect of each treatment alone (Fig. 2A and Supplementary Fig. S2A). By day 22, tumor volumes in mice treated with the combined therapy were lower than those in control mice, mice treated with the anti-PD-1 antibody or treated with the anti-C5a aptamer. Remarkably, by day 41, all the mice (n=9) in the combination group showed complete tumor rejection. In contrast, at day 48, only one mouse in the control group, two in the group treated with AON-D21 and four in the group treated with anti-PD-1 showed tumor rejection. Moreover, all these mice resisted a tumor rechallenge performed after an untreated period of eighty days, suggesting the development of an efficient antitumor long-term memory response (Supplementary Fig. S2B). We also tested the effect of the combination in a different syngeneic mouse model based on the subcutaneous implantation of Lewis lung adenocarcinoma (LLC) cells (Fig. 2B and Supplementary Fig. S2C). Anti-PD-1 treatment on days 7, 10 and 14 administered in combination with AON-D21 (every other day) resulted in an attenuation of tumor growth that became significant by day 14. Although complete rejections were not observed in this model, a survival analysis confirmed the benefit of the

combined treatment (Fig. 2C). The combination treatment was also able to increase the survival of mice following injection of LLC cells into the tail vein (Fig. 2D), suggesting that the treatment inhibited lung cancer metastasis. Lastly, C5a blockade synergized with PD-1 blockade to prevent multiorgan metastases after intracardiac injection of highly aggressive Kras-mutated lung adenocarcinoma Lacun3 cells (Fig. 2E). A survival analysis performed in an independent experiment in which anti-PD-1 treatment was ceased on day 10 confirmed the benefit of the combined treatment (Fig. 2F). In conclusion, the combined immunotherapy based on C5a and PD-1 blockade showed synergistic effects on both lung cancer growth and metastatic progression.

The antitumor activity of the combined treatment is mediated by CD8 T cells

To identify changes induced in the tumor microenvironment by C5a and/or PD-1 blockade, we analyzed the immune cells present in 393P tumor-bearing mice. By day 14, statistically significant differences in tumor size were observed between groups, and were maintained until the end of the experiment (Fig. 3A). Animals were sacrificed at day 26 before tumors were completely rejected by the combined treatment. At this point, the combined anti-C5a/PD-1 treatment resulted in a significant elevation of the percentage of CD8 T cells in the spleens of the treated animals, as compared with the control mice; while no changes were observed in other immune subpopulations (Supplementary Fig. S3). In tumors, the effect on the frequency of CD8 T cells was stronger (Fig. 3B and Supplementary Fig. S4). In addition, the combination treatment led to a decrease in the frequency of MDSC leukocyte subpopulation in tumors, as compared to the control group (Fig. 3B). None of the treatments significantly modified the frequency of CD4 T cells, NK cells or Tregs in tumors, except for a reduction of NK cells in tumors treated with the dual blockade (Supplementary Fig. S5). Further analyses revealed that in tumors treated with the dual therapy there was a negative

correlation between CD8 T cells and MDSCs, as well as an increase in CD45-positive cells per mg of tumor (Fig. 3B). In support of the relevance of MDSCs in the model, anti-PD-1 treatment in combination with MDSC depletion had a therapeutic effect similar to that observed with the anti-PD-1/anti-C5a treatment (Fig. 3C). In relation to the involvement of potential effector cells, a selective depletion of CD8 T cells completely abrogated the antitumor efficacy of the combination therapy against 393P cells (Fig. 3D). CD4 T cells and NK cells seemed to be dispensable, although in the case of NK cells a moderate growth increase was observed at the last days of the experiment, suggesting that NK cell depletion may partially hamper the antitumor effect of the therapy. Tumor-infiltrating immune cells were also analyzed in mice bearing LLC tumors treated with anti-C5a and/or anti-PD-1 agents. Results were similar to those previously obtained with 393P tumors, although in this case significant differences were not always found (Supplementary Fig. S6 and Supplementary Fig. S7A and B).

We also analyzed the mRNA expression in the tumors of a battery of immune-related mediators. In 393P tumors, we found significant differences in the expression of three molecules: IL2, LAG3 and CCL17 (Fig. 3E and Supplementary Table S2). In the LLC model, mRNA expression of the T-cell activating cytokine IL2 was consistently elevated after the combination treatment, albeit without reaching statistical significance (Supplementary Fig. S7C). Results for LAG3 and CCL17 were not consistent with those obtained in the 393P model (data not shown). From all these experiments, we conclude that the anti-PD-1/anti-C5a combination synergistically impairs tumor growth by the action of CD8 T cells in association with an elevation of IL2.

The combined anti-C5a/anti-PD-1 therapy is effective against established tumors and is associated with an activation of CD8 T cells

To better evaluate the potential of the combined therapy in a model that more closely resembles the clinical setting, we treated established 393P tumors during a defined period of time. We observed regressions in 7 out of 8 mice treated with the combination of anti-C5a (days 9, 10 and every other day until day 24) and anti-PD-1 (days 11, 14 and 18) drugs (Fig. 4A). The combined treatment resulted in a significant improvement in survival, despite the fact that after treatment termination most tumors started growing again (Fig. 4B). In an independent experiment, we analyzed the expression of surface activation markers in tumor-infiltrating CD8 T cells. In agreement with previous results, we observed an increase in the percentage of tumor CD8 T cells (Fig. 4C). Besides, these cells showed a marked reduction in the exhaustion markers PD-1, GITR and LAG-3 (Fig. 4C). PD-1 was already downregulated in those tumors treated with anti-PD-1 alone; however, the expression of the two other markers was reduced only upon the administration of the combination therapy. We also found a trend of an increase in IL2 protein expression within the tumors (Fig. 4D). In conclusion, the combination of anti-C5a/anti-PD-1 drugs shows a significant therapeutic efficacy on tumor-bearing mice. This activity seems to be associated with an increase in the expression of IL2 and an attenuated CD8 T-cell dysfunction as compared to the anti-PD-1 monotherapy.

DISCUSSION

Numerous studies are underway to identify synergistic combinations of checkpoint inhibitors with chemotherapy, radiotherapy, targeted therapy or other immunotherapy strategies (2). Many of these combinations are built on PD-1/PD-L1 inhibition, for which the presence of immunosuppressive pathways within the tumor microenvironment represents a major hurdle. In this study we provide the framework for the clinical evaluation of an innovative combination strategy, in which anti-PD-1 antibodies are administered together with drugs that inhibit C5a signaling pathways. Overall, our study demonstrates that C5a blockade greatly synergizes with anti-PD-1 inhibition in preclinical models of local and metastatic lung cancer growth. The rationale behind this approach is that the activation and expansion of effector T cells can be optimized by targeting immunosuppressive cells in the tumor microenvironment.

Previous studies performed in diverse mouse models have led to the proposal that C5a/C5aR1 inhibition may represent a novel therapeutic target for cancer (13). Among the different potential mechanisms, C5a/C5aR1 blockade could partially reverse the immunosuppressive tumor microenvironment linked to the activity of MDSCs (5,8,10). Nonetheless, in the preclinical lung cancer models of our study the anti-C5a L-aptamer AON-D21 used as monotherapy only showed modest antitumor effects. In contrast, its administration in combination with an anti-PD-1 antibody greatly influenced the antitumor immune response in a way that resulted in a remarkable antitumor activity, both in primary lung tumors and metastatic sites.

The most plausible explanation for the synergism between anti-C5a and anti-PD-1 drugs is that C5aR1 signaling mediates mechanisms that hamper the anti-tumor activity of anti-PD-1 antibodies. In agreement with this postulate, our data show that the combined treatment leads to a lower frequency of MDSCs and a higher frequency of CD8 T cells associated with a decreased expression of exhaustion markers, which suggests a more complete restoration of

CD8 T-cell effector functions. The combination treatment was also associated with an increase in the levels of IL2, a pleiotropic cytokine with a critical role in multiple aspects of CD8 T-cell activation (14). The essential role played by CD8 T cells was reinforced by the complete abrogation of the immunotherapeutic effect after depletion of these cells. Previous studies had already suggested a role of complement in the activity of tumor infiltrating CD8 T cells. Induction of a tumor-specific CD8 T-cell response was improved upon transient inhibition of the complement system (15), and a simultaneous blockade of C3aR and C5aR1 inhibited the development of breast tumors by enhancing the effector capacity of CD8 T cells (11). Interestingly, in the same study, a combined inhibition of C3aR/C5aR1 and PD-1 enhanced antitumor effects (11). Considering these studies, a direct effect of C5a blockade on CD8 T cells is also a plausible mechanism in our models, which may lead to CD8 T-cell expansion. Contrastingly, in other pathological conditions, C5aR1 signaling seemed to be essential for an optimal generation of CD8 T-cell responses (16). In regards to the potential role played by MDSCs, their contribution to the antitumor activity of the combined therapy is supported by the reduction in the percentage of these cells in some of the studied models, its negative correlation with CD8 T cells, and the biological relevance of these cells in these models. Nevertheless, we cannot completely exclude the possibility that the reduced frequency of MDSCs was a bystander finding in our experiments, since C5a inhibition, alone or in combination with PD-1 inhibition, did not always lead to significant changes. In-depth mechanistic studies are still required to properly assess the roles played by MDSCs and CD8 T cells, without excluding the involvement of other immune cells, such as NK cells or monocytes. Interestingly, a recent study has demonstrated that C5a promotes immunosuppressive responses by contributing to the expression of PD-L1 on monocytes (17).

A comparison of the two subcutaneous tumor growth models used in our study suggests a more effective antitumor immune response in the Kras-driven model of lung adenocarcinoma.

Consequently, the impact of Kras mutations on the antitumor efficacy of the combination should be addressed, as well as the potential influence of other genetic determinants leading to neoantigen generation. Further mechanistic studies would also provide guidance for the most efficient administration schedule for immune stimulation, as well as for the potential benefit of blocking other complement mediators, such as C3aR (11). The impact of the alternative receptor for C5a, C5aR2 (C5L2), which functions are still poorly understood, should also be investigated. Finally, the extension of this combination to other tumor types merits further evaluation. Its applicability to models of lung squamous cell carcinoma, the second most common subtype of lung cancer for which anti-PD-1 therapies have also shown clinical utility (1), deserves particular consideration.

A major concern in the application of immunotherapy combinations is the potentiation of adverse effects as a result of an excessive immune activation (2). It is premature to speculate about the safety of the combination presented in this study, but clinical data from the use of the C5-blocking antibody eculizumab show that safety issues associated with complement inhibition are mainly related to the blockade of C5b-mediated bacterial lysis (18). AON-D21 selectively blocks C5a and does not interfere with C5b biology despite binding to intact C5 (19,20). Such a selective blockade of C5a/C5aR1 was safe and generally well tolerated in clinical trials (21,22). The substance class of L-aptamers (Spiegelmers) was also generally safe and well tolerated in clinical phase I and IIa studies (23).

In conclusion, our work supports the notion that the efficacy of anti-PD-1 therapies is limited by their inability to fully reprogram the tumor microenvironment, which maintains other immunosuppressive mediators. In this context, C5a/C5aR1 blockade overcomes some of the resistance mechanisms, markedly improving antitumor immune responses. These findings provide support for the clinical evaluation of anti-PD-1 and anti-C5a drugs as a combination therapy for lung cancer.

METHODS

Cell lines

393P cells, derived from KrasLA1/+p53R172HΔG mice, were a generous gift from Dr. JM Kurie (The University of Texas, MD Anderson Cancer Center, Houston, TX). Lewis lung carcinoma (LLC) cells were obtained from the American Type Culture Collection. The Lacun3 cell line was previously established by our group from a chemically induced lung adenocarcinoma carcinoma and stably transfected with the luciferase gene (24). Non-transduced Lacun3 cells were used for the survival experiment. Cells were grown in RPMI 1640 supplemented with 2 mM glutamine, 10% Fetalclone (Thermo), 100 U/ml penicillin and 100 mg/ml streptomycin (Invitrogen). All cell lines were routinely tested for Mycoplasma. Cell line authentication was not routinely performed.

AON-D21 L-aptamer

AON-D21, a follow-up of previously described NOX-D19 and NOX-D20 (19,20), is a novel PEG-modified L-aptamer (Spiegelmer). revAON-D21, a Spiegelmer of the reverse AON-D21 sequence was used as negative control. Both aptamers were synthesized at NOXXON Pharma (Berlin, Germany). Methods for the evaluation of AON-D21 affinity, pharmacokinetics and inhibitory capacity are described in the Supplementary Methods section.

Mouse models and therapeutic protocols

All animal experiments were conducted in accordance with the protocols approved by the Institutional Animal Care Committee. $Kras^{LSL\text{-}G12D/+}$;$C5aR1^{+/-}$ animals were intercrossed to generate $Kras^{LSL\text{-}G12D/+}$;$C5aR1^{+}/^{+}$ or $Kras^{LSL\text{-}G12D/+}$;$C5aR1^{-/-}$ offspring. $Kras^{LSL\text{-}G12D/+}$ mice harbor a conditionally activatable allele of oncogenic mutant Kras. Intratracheal inoculation with adenoviral Cre (AdCre) led to expression of mutant Kras. Animals were followed for a period of four months. Murine 393P cells or LLC cells ($1.5x10^6$) were resuspended in 50 µl of PBS and injected subcutaneously in the right flanks of eight weeks old Sv/129 or C57BL/6J

mice, respectively. One day before and on the day of cell injection mice were treated with AON-D21 or revAON-D21 (10 mg/kg in saline, IP), and treatment was continued every other day until the end of the experiment. For combination therapy, tumor-bearing mice were treated with anti-PD-1 blocking antibody (RMP1-14, BioXcell) at days 7, 10 and 14 after cell inoculation (100 μg per mouse in PBS, IP). Depletion of $CD8^+$, $CD4^+$ or NK^+ cells was achieved by intraperitoneal injection of 100 μg of antimouse CD8α (clone 2.43; BioXcell), CD4 (clone GK1.5; BioXcel) or NK1.1 (clone PK136; BioXcell), respectively, at days 6, 11, 14, 18, 21 and 28 after cell inoculation. Irrelevant IgG (BioXcell) was administered as control. MDSCs were depleted by intraperitoneal injection of 200 μg of antimouse anti-Gr-1 (Ly6G/C; clone RB6-8C5; BioXcell) on the day of cell injection and every other day until the end of the experiment. Tumors were measured periodically and volumes were calculated by the formula $(L \times W^2)/2$, where L is the length and W is the width. Animals were euthanized when tumor diameters reached 17 mm or when they appeared under distress. The metastasis model based on LLC cells was performed by intravenous injection of $1x10^6$ cells into the tail vein of C57BL/6J mice. The multiorgan metastatic potential of luciferase-transfected Lacun3 cells was evaluated after inoculation of $2x10^5$ cells into the left cardiac ventricle of BALB/c mice as previously described (24,25). In these two metastasis models, treatments were performed as described above, except for the injections of anti-PD-1 blocking antibody, which were performed at days 3, 7 and 10 after cell inoculation. Finally, the experiments performed with established tumors (Fig. 4) were carried out as follows: subcutaneously inoculated 393P cells ($1.5x10^6$) were allowed to grow for 9 days, mice were randomized and treatment started with AON-D21 (10 mg/kg, IP) at days 9 and 10 and every other day until day 24. Anti-PD-1 blocking antibody (100 μg per mouse) was administrated at days 11, 14 and 18 after cell inoculation.

Flow cytometry analysis

Tumors and spleens from tumor-bearing mice were mechanically disaggregated as previously described (5). Erythrocytes were lysed in a buffer containing 155 mM NH_4Cl and 10 mM $KHCO_3$. Single-cell suspensions were treated with Fc block (2.4G2; BD Pharmingen) and then stained with a labeled primary antibody against mouse CD45 (30-F11; Biolegend), CD8a (53-6.7; BD Pharmigen), NK1.1 (PK136; Biolegend), CD11b (M1/70; Biolegend), Ly6C (AL21; BD Pharmingen), Ly6G (1A8; Biolegend), LAG-3 (C9B7W; Biolegend), PD-1 (29F.1A12; Biolegend) and GITR (YGITR 765; Biolegend) diluted in FACS buffer (PBS, 0.1% NaN_3, 1% BSA). Staining of CD4 T cells and Tregs was performed using a kit from eBioscience according to the manufacturer's instructions. As an example, the gating strategy for MDSCs and CD8 T cells is shown in Supplementary Fig. S8. When indicated, dead cells were excluded using Zombie NIR Fixable Viability Kit (Biolegend), and the absolute number of CD8 T cells per milligram of tumor was determined using Cytognos Perfect Microspheres (Cytognos). Cells were acquired using a BD Biosciences FACSCalibur flow cytometer, except for the analysis of LAG-3, GITR, and PD-1 expression on CD8 T cells, which was performed on a FACSCANTO II flow cytometer. Data were analyzed using BD CellQuest Pro (BD Biosciences) and FlowJo software (Tree Star).

Immunohistochemistry

Immunohistochemistry was performed on formalin-fixed paraffin-embedded tissue sections. After antigen retrieval with EDTA buffer (CD3 and Ki67) or citrate buffer (cleaved caspase-3 and CD31), sections were incubated with the primary antibodies (anti-CD3, 1:300, Thermo Scientific; anti-Ki67, 1:100, Neomarkers; anti-cleaved caspase-3, 1:100, Cell Signaling; anti-CD31, 1:20, Dianova) overnight at 4ºC, and revealed with the EnVision HRP System (Dako) and diaminobenzidine. Quantification of staining was performed either automatically (Ki67, cleaved caspase-3 and CD31) or manually (CD3).

Expression of immune molecules within the tumors

Portions of ~0.1 cm^3 were cut from the edge of tumors, frozen in dry ice, and maintained at -80˚C until extraction. mRNA expression was evaluated by real-time PCR as previously described (5). For protein analysis, frozen tumors were lysed in an extraction buffer (100 mM Tris, 150 mM NaCl, 1 mM EGTA, 1 mM EDTA, 1% Triton X-100, 0.5% sodium deoxycholate, pH 7.4) containing a cocktail of protease inhibitors. Extracts were analyzed using the OptEIA mouse IL2 ELISA kit (BD Biosciences).

Statistical analyses

For dot plots, individual results and median per group are shown. For tumor volumes, the mean ± SEM is depicted. Comparisons between two groups were performed using the Mann-Whitney U-test. Comparisons between treatment strategies and between immune-regulator levels were performed using the Kruskal-Wallis test with the Mann-Whitney U-test as the post hoc test. Survival curves were generated using the Kaplan-Meier method, and differences were analyzed with the log rank test. For these analyses, survival times were defined as the number of days from the inoculation of the cells until the mice were euthanized or expired naturally. Spearman's rank correlation test was performed to analyze association. Significances in tumor volumes and survival tests were always calculated versus the control group. $P<0.05$ was considered significant. Statistical analyses were performed using Prism software (GraphPad).

AUTHORS' CONTRIBUTIONS

Conception and design: DA, LMM and RP

Acquisition of data: DA, SOE, HM, TL, MJP, JA, CV, AV, SV, FL, RP

Analysis and interpretation of data: All authors

Writing, review, and/or revision of the manuscript: All authors

ACKNOWLEDGEMENTS

We are grateful to Ignacio Melero for critically reviewing the manuscript. We thank Carolina Zandueta, Cristina Sainz and Amaya Lavín for technical assistance, Jonathan M. Kurie (The University of Texas, MD Anderson Cancer Center, Houston, TX) for the generous gift of 393P cells, and Diego Alignani (Cytometry Platform, CIMA), Noelia Casares and Sandra Hervas-Stubbs (Program in Immunology and Immunotherapy, CIMA) for their help with flow cytometry. The authors would also like to thank the following individuals at Noxxon Pharma: Lucas Bethge (chemical synthesis of AON-D21, revAON-D21 and hybridization probe for bioanalysis), Christian Maasch (AON-D21 affinity determination and bioanalysis from mouse pharmacokinetics by surface plasmon resonance experiments), Klaus Buchner and Dirk Zboralski (cell-based potency assays).

REFERENCES

1. Brahmer J, Reckamp KL, Baas P, Crinò L, Eberhardt WEE, Poddubskaya E, et al. Nivolumab versus docetaxel in advanced squamous-cell non-small-cell lung cancer. N Engl J Med 2015;373:123-35.
2. Melero I, Berman DM, Aznar MA, Korman AJ, Pérez Gracia JL, Haanen J. Evolving synergistic combinations of targeted immunotherapies to combat cancer. Nat Rev Cancer 2015;15:457-72.
3. Youn J-I, Nagaraj S, Collazo M, Gabrilovich DI. Subsets of myeloid-derived suppressor cells in tumor-bearing mice. J Immunol 2008;181:5791-802.
4. Mkrtichyan M, Najjar YG, Raulfs EC, Abdalla MY, Samara R, Rotem-Yehudar R, et al. Anti-PD-1 synergizes with cyclophosphamide to induce potent anti-tumor vaccine effects through novel mechanisms. Eur J Immunol 2011;41:2977-86.
5. Corrales L, Ajona D, Rafail S, Lasarte JJ, Riezu-Boj JI, Lambris JD, et al. Anaphylatoxin C5a creates a favorable microenvironment for lung cancer progression. J Immunol 2012;189:4674-83.
6. Berraondo P, Minute L, Ajona D, Corrales L, Melero I, Pio R. Innate immune mediators in cancer: between defense and resistance. Immunol Rev 2016;274:290-306.
7. Pio R, Ajona D, Lambris JD. Complement inhibition in cancer therapy. Semin Immunol 2013;25:54-64.
8. Markiewski MM, DeAngelis RA, Benencia F, Ricklin-Lichtsteiner SK, Koutoulaki A, Gerard C, et al. Modulation of the antitumor immune response by complement. Nat Immunol 2008;9:1225-35.
9. Sharma SK, Chintala NK, Vadrevu SK, Patel J, Karbowniczek M, Markiewski MM. Pulmonary alveolar macrophages contribute to the premetastatic niche by suppressing antitumor T cell responses in the lungs. J Immunol 2015;194:5529-38.

10. Vadrevu SK, Chintala NK, Sharma SK, Sharma P, Cleveland C, Riediger L, et al. Complement C5a receptor facilitates cancer metastasis by altering T cell responses in the metastatic niche. Cancer Res 2014;74:3454-65.
11. Wang Y, Sun S-N, Liu Q, Yu Y-Y, Guo J, Wang K, et al. Autocrine complement inhibits IL10-dependent T-cell mediated antitumor immunity to promote tumor progression. Cancer Discov 2016;6:1022–35.
12. Gibbons DL, Lin W, Creighton CJ, Rizvi ZH, Gregory PA, Goodall GJ, et al. Contextual extracellular cues promote tumor cell EMT and metastasis by regulating miR-200 family expression. Genes Dev 2009;23:2140-51.
13. Pio R, Corrales L, Lambris JD. The role of complement in tumor growth. Adv Exp Med Biol 2014;772:229-62.
14. Boyman O, Sprent J. The role of interleukin-2 during homeostasis and activation of the immune system. Nat Rev Immunol 2012;12:180-90.
15. Janelle V, Langlois M-P, Tarrab E, Lapierre P, Poliquin L, Lamarre A. Transient complement inhibition promotes a tumor-specific immune response through the implication of natural killer cells. Cancer Immunol Res 2014;2:200-6.
16. Kim AHJ, Dimitriou ID, Holland MCH, Mastellos D, Mueller YM, Altman JD, et al. Complement C5a receptor is essential for the optimal generation of antiviral CD8+ T cell responses. J Immunol 2004;173:2524-9.
17. An L-L, Gorman J V, Stephens G, Swerdlow B, Warrener P, Bonnell J, et al. Complement C5a induces PD-L1 expression and acts in synergy with LPS through Erk1/2 and JNK signaling pathways. Sci Rep 2016;6:33346.
18. Ward PA, Guo R-F, Riedemann NC. Manipulation of the complement system for benefit in sepsis. Crit Care Res Pract 2012;2012:427607.
19. Yatime L, Maasch C, Hoehlig K, Klussmann S, Andersen GR, Vater A. Structural

basis for the targeting of complement anaphylatoxin C5a using a mixed L-RNA/L-DNA aptamer. Nat Commun 2015;6:6481.

20. Hoehlig K, Maasch C, Shushakova N, Buchner K, Huber-Lang M, Purschke WG, et al. A novel C5a-neutralizing mirror-image (L-)aptamer prevents organ failure and improves survival in experimental sepsis. Mol Ther 2013;21:2236-46.

21. Sun S, Zhao G, Liu C, Fan W, Zhou X, Zeng L, et al. Treatment with anti-C5a antibody improves the outcome of H7N9 virus infection in African green monkeys. Clin Infect Dis 2015;60:586-95.

22. Jayne DR, Bruchfeld A, Schaier M, Ciechanowski K, Harper L, Jadoul M, et al. OP0227 oral C5a receptor antagonist CCX168 phase 2 clinical trial in ANCA-associated renal vasculitis. Ann Reum Dis 2014;73:148.

23. Vater A, Klussmann S. Turning mirror-image oligonucleotides into drugs: the evolution of Spiegelmer(®) therapeutics. Drug Discov Today 2015;20:147-55.

24. Bleau A-M, Freire J, Pajares MJ, Zudaire I, Anton I, Nistal-Villán E, et al. New syngeneic inflammatory-related lung cancer metastatic model harboring double KRAS/WWOX alterations. Int J Cancer 2014;135:2516-27.

25. Antón I, Molina E, Luis-Ravelo D, Zandueta C, Valencia K, Ormazabal C, et al. Receptor of activated protein C promotes metastasis and correlates with clinical outcome in lung adenocarcinoma. Am J Respir Crit Care Med 2012;186:96-105.

FIGURE LEGENDS

Figure 1. C5aR1 genetic deficiency and C5a pharmacological blockade decreases lung tumor burden. **A**, Representative H&E-stained lung sections from $Kras^{LSL\text{-}G12D/+}$ (n=24) and $Kras^{LSL\text{-}G12D/+}$;$C5aR1^{-/-}$ mice (n=18) treated with AdCre and allowed to develop tumors for four months. **B**, Quantification of number of tumors per mouse and tumor areas. Data correspond to two independent experiments. **C**, Flow cytometric analysis of splenic CD11bLy6C MDSCs. **D**, Immunohistochemical evaluation of CD3-positive cells in the lung tumors (n=12 per group) with two representative images. Scale bar, 30 μm. **E**, Kaplan-Meier survival curves of $Kras^{LSL\text{-}G12D/+}$ (n=14) and $Kras^{LSL\text{-}G12D/+}$;$C5aR1^{-/-}$ (n=13) mice from an independent experiment. **F**, Tumor growth of 393P cells injected subcutaneously into syngeneic Sv/129 mice treated with the C5a antagonist AON-D21 (n=8) or the negative control revAON-D21 (n=7). **G**, Flow cytometric analysis of splenic MDSCs from 393P tumor-bearing mice on day 40. **P*<0.05; ***P*<0.01.

Figure 2. Combined blockade of PD-1 and C5a decreases lung tumor burden and metastatic progression. **A**, Tumor growth of 393P cells implanted subcutaneously in syngeneic Sv/129 mice treated with anti-C5a (every other day), anti-PD-1 (days 7, 10, 14), or both (9 mice per group). **B**, Tumor growth of LLC cells injected subcutaneously in syngeneic C57BL/6J mice treated as above (8 mice per group), and Kaplan-Meier survival curves of these mice (**C**). **D,** Kaplan-Meier survival curves after intravenous injection of LLC tumors into the tail vein of mice treated as indicated. **E**, Bioluminescence quantitation after intracardiac inoculation of syngeneic Lacun3 cells in BALB/c mice treated with anti-C5a (every other day), anti-PD-1 (days 3, 7 and 10) or both (6-7 mice per group). Light was measured at day 0, at day 7 and at the end of the experiment (day 14). A representative mouse from each treatment group (at days 7 and 14) are shown. Dot plot shows the relative change of bioluminescence between days 0 and 14. At day 7, no significant changes were still observed between groups (data not

shown). **F**, Kaplan-Meier survival curves from an independent experiment of mice inoculated in the left cardiac ventricle with naïve Lacun3 cells non-transduced with luciferase and treated as indicated (9-10 mice per group). In all the experiments of this figure revAON-D21 was used in the control group. *P<0.05; ***P<0.001.

Figure 3. The antitumor activity observed after the C5a and PD-1 blockade is mediated by CD8 T cells. **A**, Tumor growth of 393P cells in mice treated with AON-D21, anti-PD-1, or their combination for endpoint flow cytometry analysis (n=8 per group). RevAON-D21 was used as control. **B**, Flow cytometric analysis of CD8 T cells, MDSCs and CD45-positive cells (n=4 per group) in tumors harvested at day 26. The correlation between CD8 T cells and MDSCs in the combined group is also shown. Spearman's rank correlation test was performed to analyze the association. Data on CD45-positive cells per mg of tumor were generated in an independent experiment. **C**, Tumor growth of 393P cells in mice treated as indicated with and without MDSC depletion with anti-Gr-l. RevAON-D21 was used as negative control and anti-C5a/anti-PD-1 as positive control. Five mice were used per group. Statistically significant differences in tumor volume at the end of the experiment are shown. **D**, Tumor growth of 393P cells in mice treated with revAON-D21 (control), the anti-C5a/anti-PD-1 combination, and the combination in the presence of depleting antibodies against CD8, CD4 or NK cells. An additional control group consisting of mice treated with revAON-D21 and an irrelevant IgG was used, but not shown for the sake of clarity since no differences were observed between control groups. Five mice were used per group. Statistically significant differences in tumor volume at the end of the experiment are shown. **E**, IL2 mRNA levels in 393P tumors determined by real-time PCR and expressed as relative to β-actin mRNA. *P<0.05; **P<0.01; ***P<0.001.

Figure 4. Combined C5a and PD-1 blockade is able to control the growth of established tumors in association with an activation of CD8 T cells. **A**, Subcutaneously injected 393P

cells were allowed to grow for 9 days and mice were randomized into four groups (eight-nine mice per group). Mice were treated with anti-C5a (days 9, 10 and every other day until day 24), with anti-PD-1 (days 11, 14 and 18) or both. Mice in the control group were treated with revAON-D21. The waterfall plot shows the responses to treatment as measured between treatment initiation (day 9) and one day after treatment termination (day 25). **B**, Kaplan-Meier survival curves of these mice. The experiment was terminated when all mice with growing tumors died. The statistical significance corresponds to the comparison between the control group and the combined treatment. **C**, Flow cytometric analysis of CD8 T cells and exhaustion markers PD-1, GITR and LAG-3 (expressed as mean fluorescence intensity on CD8 T cells) in 393P tumors grown in mice treated as above in an independent experiment terminated at day 19. For this analysis, dead cells were excluded using Zombie NIR Fixable Viability Kit. Four animals were used per group. Of note, one of the mice treated with the combination anti-C5a/anti-PD-1 showed a complete remission of the tumor and, consequently, could not be analyzed (which deterred us to perform a statistical analysis of the data). **D**, IL2 protein levels in these tumors. *P<0.05; **P<0.01; ***P<0.001.

Author Manuscript Published OnlineFirst on March 13, 2017; DOI: 10.1158/2159-8290.CD-16-1184
Author manuscripts have been peer reviewed and accepted for publication but have not yet been edited.

FIGURE 1

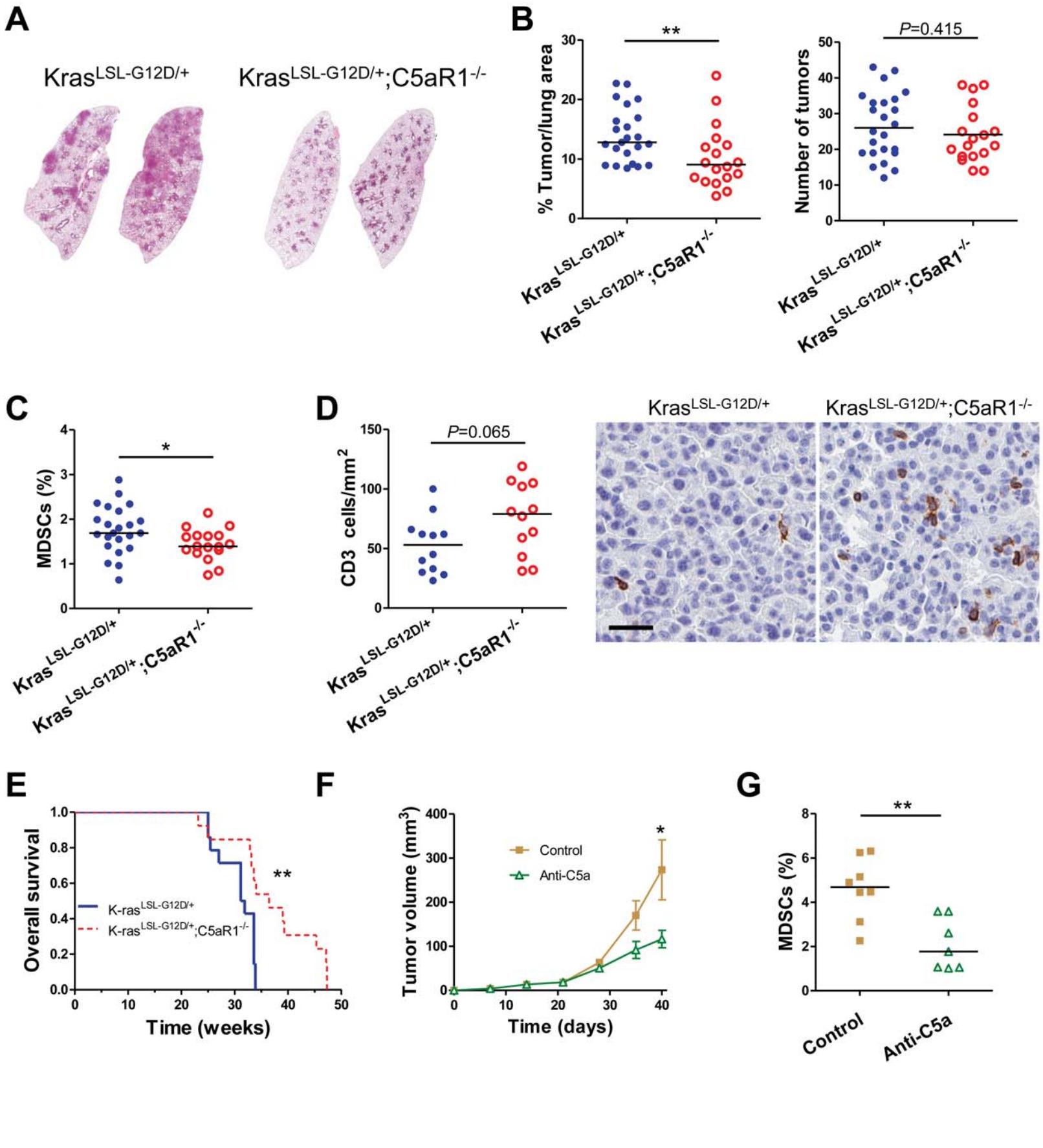

FIGURE 2

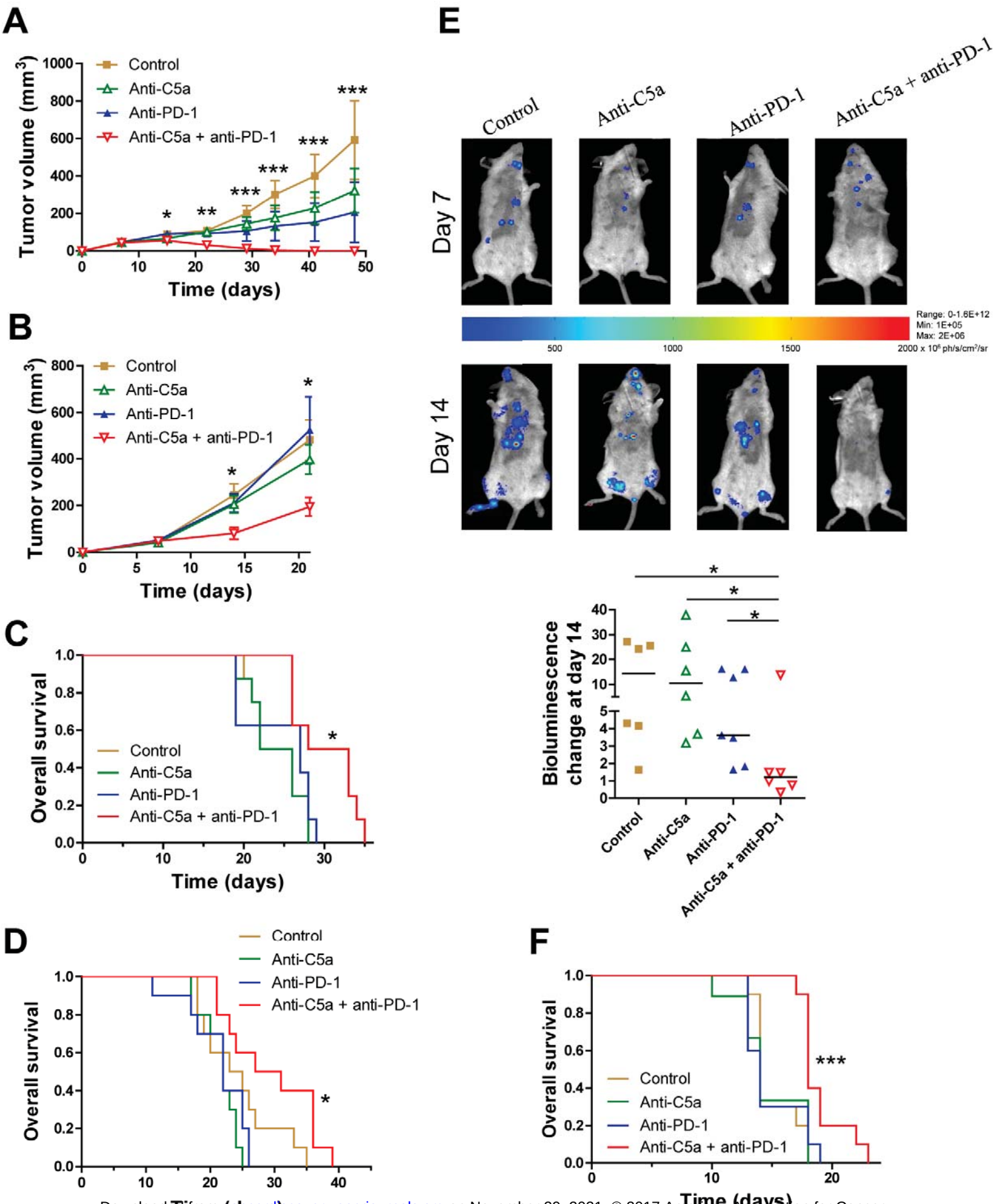

Author Manuscript Published OnlineFirst on March 13, 2017; DOI: 10.1158/2159-8290.CD-16-1184
Author manuscripts have been peer reviewed and accepted for publication but have not yet been edited.

FIGURE 3

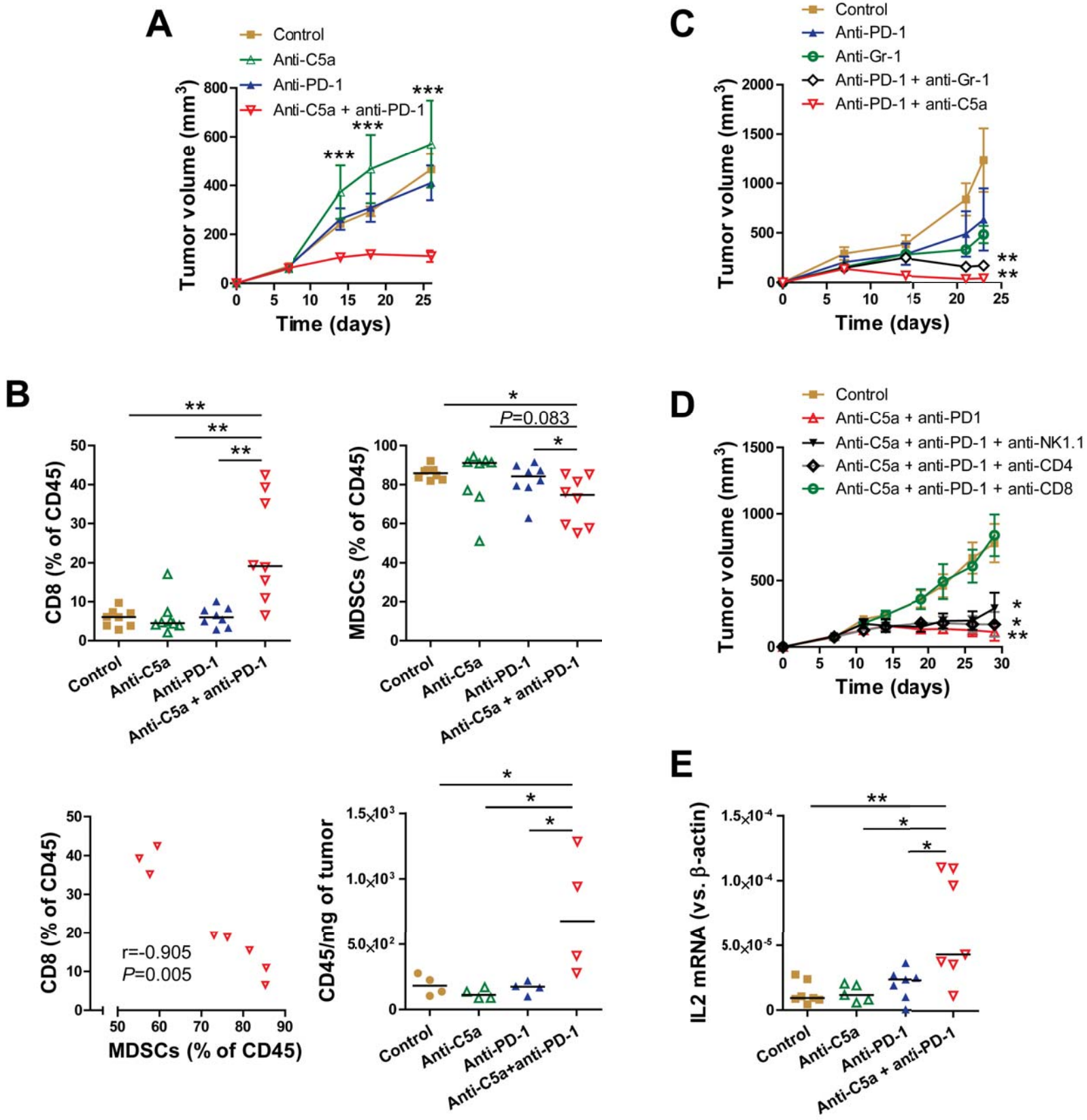

Author Manuscript Published OnlineFirst on March 13, 2017; DOI: 10.1158/2159-8290.CD-16-1184
Author manuscripts have been peer reviewed and accepted for publication but have not yet been edited.

FIGURE 4

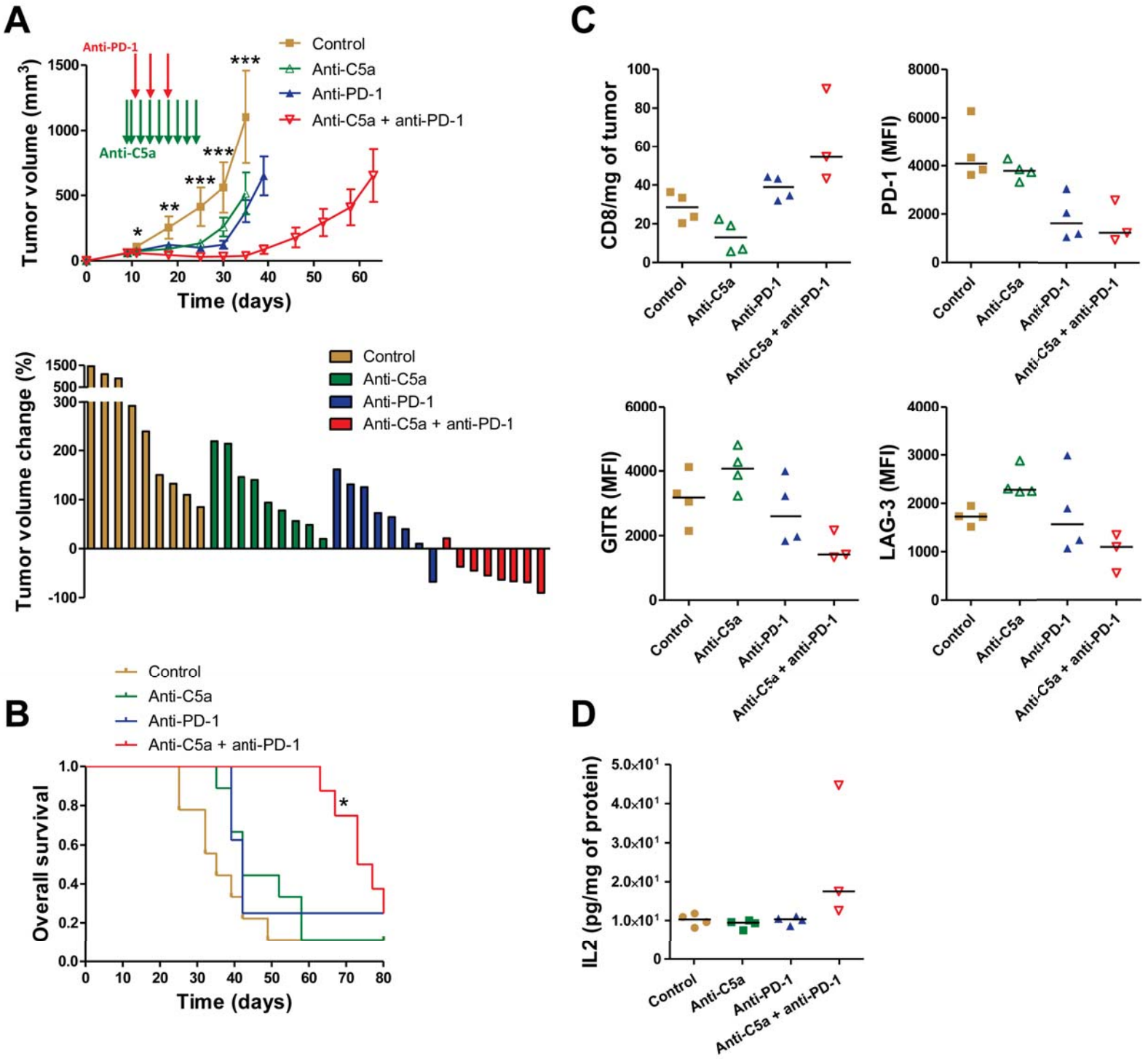

AACR American Association for Cancer Research

CANCER DISCOVERY

A Combined PD-1/C5a Blockade Synergistically Protects Against Lung Cancer Growth and Metastasis

Daniel Ajona, Sergio Ortiz-Espinosa, Haritz Moreno, et al.

Cancer Discov Published OnlineFirst March 13, 2017.